Rapid Communications

Probing strain modulation in a gate-defined one-dimensional electron system

M. H. Fauzi,[1,*] M. F. Sahdan,[2] M. Takahashi,[2] A. Basak,[3] K. Sato,[2] K. Nagase,[2] B. Muralidharan,[3] and Y. Hirayama[1,2,4,†]

[1]*Center for Spintronics Research Network, Tohoku University, Sendai 980-8577, Japan*

[2]*Department of Physics, Tohoku University, Sendai 980-8578, Japan*

[3]*Department of Electrical Engineering, Indian Institute of Technology Bombay, Mumbai 400076, India*

[4]*Center for Science and Innovation in Spintronics (Core Research Cluster), Tohoku University, Sendai 980-8577, Japan*

(Received 14 January 2019; revised manuscript received 15 October 2019; published 2 December 2019)

Gate patterning on semiconductors is routinely used to electrostatically restrict electron movement into reduced dimensions. At cryogenic temperatures, where most studies are carried out, differential thermal contraction between the patterned gate and the semiconductor often lead to an appreciable strain modulation. The impact of such modulated strain to the conductive channel buried in a semiconductor has long been recognized, but measuring its magnitude and variation are rather challenging. Here we present a way to measure that modulation in a gate-defined GaAs-based one-dimensional channel by applying resistively detected NMR with *in situ* electrons coupled to quadrupole nuclei. The detected strain magnitude, deduced from the quadrupole-split resonance, varies spatially on the order of 10^{-4}, which is consistent with the predicted variation based on an elastic strain model. We estimate the initial lateral strain ϵ_{xx} and ϵ_{yy} developed at the interface to be about 5.0×10^{-3}.

DOI: 10.1103/PhysRevB.100.241301

In many semiconductor-based quantum systems, electrons are manipulated by applying voltages to the surface metal gates. For example, a combination of nanoscale metal gates and GaAs-based two-dimensional systems enables us to realize one-dimensional quantum channel and zero-dimensional quantum dot by depleting electrons under the gates [1]. These building blocks are integrated into many quantum devices, such as quantum computing/simulating systems based on electron spins [2–4]. Electron control in these systems is always accompanied by an electron position change from the originally two-dimensional sheet. One can expect microscopic strain distribution in such devices because surface metal gates and semiconductor systems have different thermal expansion coefficients and complicated nanometer surface gates should produce a complicated strain pattern inside. Such phenomena are common for all semiconductor systems including silicon and other semiconductor groups. However, the strain variation felt by confined electrons has not received much attention up to now partly because of a lack of an appropriate and precise measurement tool to probe local strain in a nanometer-scale electron channel. Here, taking GaAs-based quantum point contact (QPC) [5,6] as a prototypical example, we demonstrate that electrons flowing in the one-dimensional channel feel different strain even in the same device when the channel position is microscopically shifted by changing the gate voltage.

There are a couple of methods to measure spatial strain distribution in materials. Examples include x-ray diffraction [7,8], electron microscopy [9,10], and Raman spectroscopy [11–13]. Although those techniques are capable of delivering a high-spatial-resolution strain profile, they are only sensitive to strain magnitude larger than a factor of 10^{-4}. An alternative technique such as solid-state NMR could provide an acceptable solution since it has the ability to detect ultra-low-level strain variation of less than 10^{-4} through nuclear quadrupolar interaction with the electric field gradient [14–16]. However, macroscopic samples are needed for the conventional NMR detection technique to work. Furthermore, it is difficult to get information of the electron-existing nanometer-scale area inside the semiconductors with these techniques.

To overcome the limitation, the so-called optically detected (or optically pumped) NMR with quadrupole nuclei has been developed and exploited intensively to investigate structural information of strained semiconductor nanostructures [17–26]. However, this technique requires an interrogated structure to be optically accessible, which cannot be easily applied to nanostructure transport devices defined by surface gate metals such as quantum point contacts [5,6] or lateral surface superlattices [27–29]. To circumvent the difficulties, we utilize a resistively detected NMR (RDNMR) technique where both nuclear-spin polarization and detection can be realized in the electron channel thanks to the successful RDNMR in QPCs [30,31].

In this experiment, we used a QPC defined by three independent metallic gates placed on the semiconductor top [31] as depicted in Fig. 1(a). In the RDNMR experiment, we applied a perpendicular magnetic field, which pushed the system into the quantum Hall regime with edge channels. To avoid a possible reflection from the center gate arm connected to the outside of the Hall bar, we fully depleted the electron channel

*Present address: Research Center for Physics, Indonesian Institute of Sciences, South Tangerang City, Banten 15314, Indonesia; moha065@lipi.go.id

†yoshiro.hirayama.d6@tohoku.ac.jp

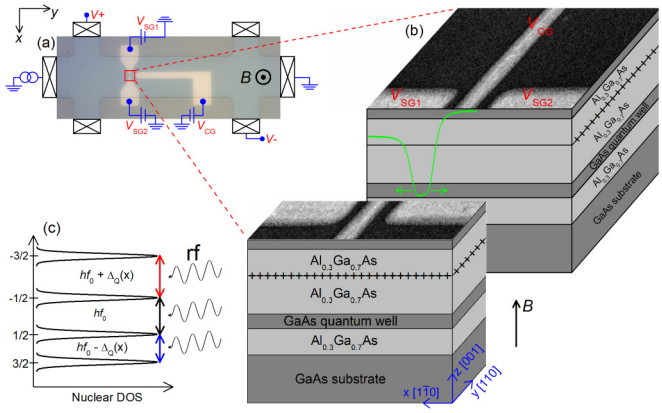

FIG. 1. (a) An optical image of the device layout and transport measurement schematic. Cross marks indicate the Ohmic contact pads. (b) A scanning electron microscopy image of the fine metal gates along with a schematic of the cut-through wafer structure. An array of plus signs drawn in between the AlGaAs layer indicates a Si delta doping. The lithographic gap (width) between (of) V_{SG1} and V_{SG2} is 600 (500) nm. The center metal gate V_{CG} has a lithogarphic width of 200 nm. Applying negative bias voltages to those gates defines the confinement potential (green curve) and controls the channel position in the lateral direction indicated by the green arrow. The center gate deposited in between the pair of split gates gives us more freedom to tune the confinement potential and thereby allows us to shift the channel over a wider region along the x direction than that offered by a traditional point contact device with a pair of split gates only. (c) Anisotropic strained lattices, whose values are positional dependent, create an electric field gradient. An energy level of a 3/2 quadrupole nuclei in close proximity to the field gradient would be affected and can be observed directly through the NMR spectrum.

between the center gate and split gate 2 by applying a negative bias voltage to V_{SG2}, which is more negative than a pinch-off bias voltage, naturally depending on a bias applied to the center gate, V_{CG} [32]. Figure 1(b) shows a three-dimensional schematic view of the electron channel in the QPC. The wafer structure used here puts a two-dimensional electron plane at 175 nm from the surface. The quasi-one-dimensional QPC channel is defined by a combination of negative V_{SG1} (voltage applied to split gate 1) and V_{CG}. The channel position can be laterally shifted by tuning V_{SG1} and V_{CG} as schematically shown in Fig. 1(b), thereby allowing us to selectively polarize the nuclear spins in certain areas of the GaAs layer. We start off with the condition where the electron channel locates around the edge of split gate 1. We can expect a large strain slope in this situation. Based on many experiments done with different gate voltages, we found that the expected situation can be obtained by applying $V_{CG} = -0.45$ V.

Before going into the detailed experimental results, we will discuss how we obtained the RDNMR signal in the electron channel. Dynamic nuclear polarization (DNP) relied on the hyperfine-mediated interedge spin-flip scattering within the same Landau level as described in our previous theoretical and experimental studies [31,33]. We applied the 4.5 T magnetic field perpendicular to the sample to reach the lowest Landau level (filling factor $\nu = 2$) at a lattice temperature of 300 mK. Note that although we cooled the sample down to a subkelvin temperature, it is not strictly required since the technique relies on the breakdown of the integer quantum Hall effect [34]. DNP was induced by applying an ac bias current of about 10 nA for more than 1500 s at a certain point along the red conductance traces [see Fig. 2(a)], corresponding to the filling factor less than 1 ($\nu < 1$) in the constriction. This was followed by slowly scanning rf with increasing frequency through home-made coils wound around the device with a rf power of -30 dBm delivered to the top of the cryostat and a scanning speed of 100 Hz/s. All the spectra were acquired in a single shot measurement and we kept gate bias voltages fixed throughout the sequences [35]. The QPC conductance is determined by the highest potential at the center of the constriction so that any slight change of the potential height by nuclear Zeeman energy can be sensitively detected in RDNMR. In our previous study in Ref. [31], we confirmed that the RDNMR signals were Knight shifted, proving that the detected signals came from inside the constriction where ν is close to 1.

As already mentioned, we applied $V_{CG} = -0.45$ V to the center metal gate, and then repeated current-induced dynamic nuclear polarization and RDNMR measurements at a certain range of V_{SG1} bias voltage along the red line as indicated in the magnetotransport traces displayed in Fig. 2(a). A represented ^{75}As RDNMR spectrum shown in the inset of Fig. 2(b) exhibits threefold splitting due to nuclear quadrupole interaction with the strain field [36]. We extracted the average quadrupole splitting value for each obtained RDNMR spectrum with a Gaussian fit. The extracted values are displayed in Fig. 2(b). The detected splitting was initially about 10 kHz at a bias voltage of $V_{SG1} = -0.7$ V with the center of each transition peak being slightly convoluted but still recognizable. However, by applying more negative bias voltage to V_{SG1}, the splitting between the center and satellite peaks progressively increased, reaching up to about 25 kHz at $V_{SG1} = -1.1$ V. For the case of $V_{CG} = -0.45$ V, this increased splitting clearly indicates that electrons in the channel feel different strain when the channel is laterally shifted. Although this result was expected, here we clearly indicate that a slight change in the voltage condition considerably changes the strain in the channel, even within a single QPC device.

To discuss more quantitatively, we estimate strain distribution in our QPC device with three metallic gates placed on the semiconductor top as depicted in Fig. 1(a). Each metal gate exerts a stress on the semiconductor due to different coefficients of thermal expansion; correspondingly, the resultant of the stressors produces a lateral strain field modulation in the channel. To quantitatively assess the strain profile in our channel, we use COMSOL MULTIPHYSICS FEM package [37]. Figure 3 displays the simulated lateral strain profile $\epsilon_{tot} = \epsilon_{zz} - (\epsilon_{xx} + \epsilon_{yy})/2$, located 175 nm below the surface. The initial strain at the interface is set to be $\epsilon^0_{xx} = 5 \times 10^{-3}$, $\epsilon^0_{yy} = 5 \times 10^{-3}$, and $\epsilon^0_{zz} = 0$. The corresponding quadrupole splitting Δ_Q is given by

$$\Delta_Q = \frac{eQS_{11}}{2h}\epsilon_{tot}, \tag{1}$$

where e is the elementary charge and h is the Planck constant. We use a recent refined value of the product of the nuclear quadrupole moment Q and S-tensor diagonal

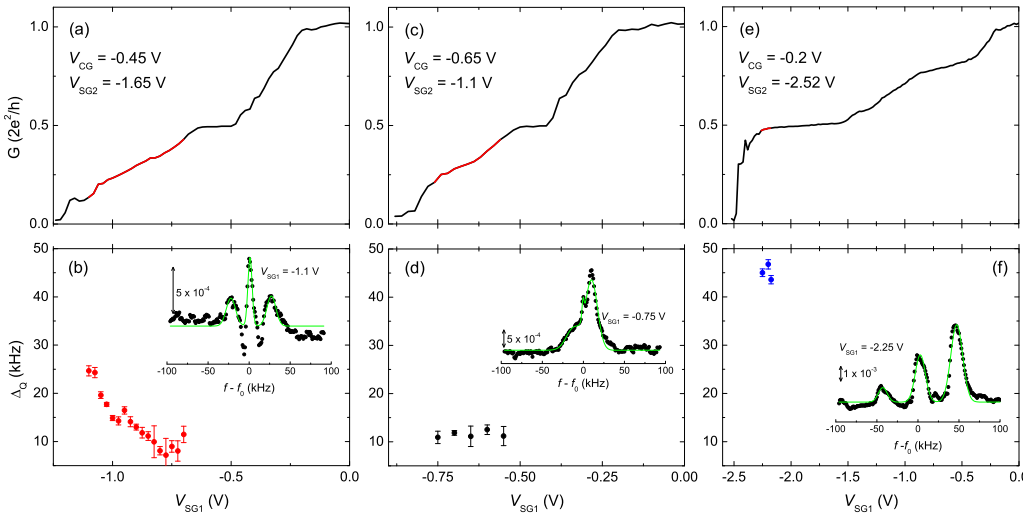

FIG. 2. (a),(c),(e) Upper panel from left to right shows diagonal magnetotransport trace as a function of the left-hand-side split gate (V_{SG1}) with ($V_{SG2} = -1.65$ V, $V_{CG} = -0.45$ V), ($V_{SG2} = -1.1$ V, $V_{CG} = -0.65$ V), and ($V_{SG2} = -2.52$ V, $V_{CG} = -0.2$ V). (b),(d),(f) Lower panel shows quadrupole splitting Δ_Q from the RDNMR spectra measured along the red line in the upper conductance panel. The inset in each panel shows a represented spectrum.

component $QS_{11} = +0.758 \times 10^{-6}$ V for ^{75}As nuclei [38], which is about 1.4 smaller than the value derived earlier by Sundfors *et al.* [39].

As plotted in Fig. 3, the strain distribution to the left ($x < 0$) and to the right ($x > 0$) sides of the center gate is identical. But, we use only the left side in our present experiments. Around the edge of the split metal gate shown in (ii) in Fig. 3, the Δ_Q ranges from 0 to 30 kHz, showing good consistency with the experimental results obtained in Fig. 2(b).

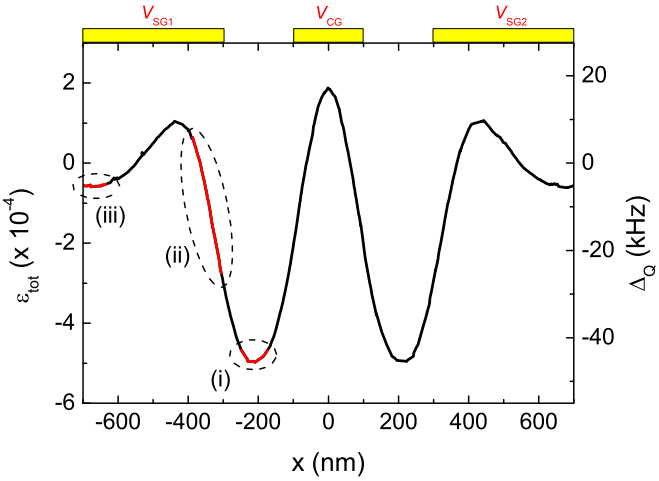

FIG. 3. Calculated total strain field modulation ϵ_{tot} and corresponding quadrupole splitting Δ_Q felt by a ^{75}As nuclei located 175 nm below the surface. The strain profile has a mirror symmetry at $x = 0$. Three distinct regions of interest, which are accessible experimentally, are highlighted alphabetically. The total strain reaches a maximum value halfway between the split and center gates, corresponding to region (i). The strain drops rather quickly towards the left split gate (SG1) and changes its sign. The profile is inflected at $x = -440$ nm and the value slowly reduces toward the far left split metal gate (SG1).

To further confirm our understanding, next, we set $V_{CG} = -0.65$ V as displayed in Figs. 2(c) and 2(d). The electron channel pushed far underneath split metal gate 1 in this condition. Current-induced DNP and RDNMR measurements were carried out at a certain range of V_{SG1} bias voltage along the red line as indicated in the magnetotransport traces displayed in Fig. 2(c). The extracted quadrupole splitting within the measurement range is displayed in Fig. 2(d) with a typical ^{75}As RDNMR spectrum shown in the inset. The splitting was consistent around 10 kHz, unchanged throughout the bias voltage range of interest. This suggests that the nuclear spins were polarized in a small and also less modulated strained region indicated by (iii) in Fig. 3.

On the other hand, we also try to reduce the applied bias voltage to the center gate to $V_{CG} = -0.2$ V to be able to approach the strain field in the exposed area halfway in between the left-hand side split and center metal gates [(i) in Fig. 3], where according to our model, a maximum strain field is expected. Unlike the other two former cases, we notice that the conductance quickly went to zero after passing through the last half-integer plateau as shown in Fig. 2(e). This occurred because the channel width was already too narrow and consequently we could only accumulate a limited number of spectra to the left vicinity of the plateau, indicated by the red-colored trace. As shown in the inset of Fig. 2(f), each peak was clearly separated since the splitting, of about 45 kHz, has already exceeded the linewidth of each resonance peak. From the splitting value and the channel narrowness, we estimate the nuclear spin polarization detected occupying a volume of around $100 \times 500 \times 20$ nm^3, involving about 10^7 nuclear spins. Since each peak intensity was clearly deconvoluted, the nuclear spin temperature could be estimated easily from the ratio of two satellite intensities [40] of around -2 mK, indicating that the nuclear spins are population inverted. The net nuclear spin polarization in the point contact was increased by current-induced DNP, so that the nuclear spins were expected to be far from equilibrium [41,42]. The

detected spectrum was similar to the calculated RDNMR response for relatively large and homogeneously strained ^{75}As atoms [33]. This is in contrast with the other two former cases where the center transition intensities were mostly found to be more pronounced. Reference [26] argues that the more pronounced center transition intensity is likely because the nuclear spin polarization spreads over to the unstrained ^{75}As atoms. To clearly identify them, it requires a more elaborate two-dimensional strain modeling in combination with self-consistent electron density distribution calculation.

Other possible strain sources such as sample mounting onto a chip carrier and lattice mismatch do contribute to the overall signal we observed. However, the contribution was negligibly small than that due to differential thermal contraction between the fine metal gates and GaAs semiconductor [43]. A similar result was also reported for a 10-μm-wide Hall bar based on a high-mobility GaAs wafer where sample mounting, lattice mismatch, and global surface gate covering the entire Hall bar had negligible contributions to the ^{75}As quadrupole splitting [44]. In addition to that, the electric field from the gates could couple to the quadrupole moment via the piezoelectric effect as discussed in Refs. [22,45–48]. In our case, however, the piezoelectric effect did not contribute to the field gradient. This is because the external electric field only coupled to the d_{31} piezoelectric tensor component [49], thus only producing a shear strain component.

In summary, we have demonstrated a direct detection of the built-in strain modulation on the order of 10^{-4} in the nanometer-scale channel by electrical means and identified different strain regions. The detection was possible in part since we were able to guide the spin-polarized edge current pathways to a different portion of the channel by gate bias tuning. The sensitivity of our strain measurement is currently limited by the center transition linewidth broadening of more than 10 kHz due to the coupling via inhomogeneous Knight field reflecting electron density distribution in the channel [50]. However, it is possible to improve the detection sensitivity by a factor of 5 at most by depleting the electron density in the channel after each DNP cycle as described in Refs. [50,51]. One can then reduce the central transition linewidth to be as small as 2 kHz [50], the lower limit due to the nuclear dipolar interaction.

Evaluation of strain field and its distribution sensed by electrons in a single gate-defined nanostructure is important to understand transport phenomena better in mesoscopic systems as it may alter the confinement potential shape either via deformation potential or piezoelectric coupling [28]. This is particularly relevant for a shallow conductive channel involving multiple gate arrays to study a transport anomaly such as the enigmatic 0.7 structures in quantum point contacts, which proved to be sensitive to the confinement potential profile [52–54].

Beyond GaAs, one can apply the technique to other semiconductor compounds. In fact, quadrupole-split resistively detected NMR or ESR has been observed in an InSb- [55] or InAs- [56] based two-dimensional electron system. They both attribute the origin of the splitting due to lattice mismatch. However, electrostatically defined quantum point contacts with a fine surface gating on InSb and InAs compounds are still considered to be technologically challenging, either due to the presence of parasitic conductance or charge trapping. However, Mittag *et al.* recently has addressed some of the issues and they were able to observe a clear one-dimensional conductance quantization [57].

Recently Jouan *et al.* has succeeded in fabricating a gate-defined quantum point contact based on $LaAlO_3/SrTiO_3$ transition metal oxide compounds [58], a material that surprisingly exhibits a strong change in the transport properties in response to mechanical bending or stretching [59]. The compounds have two active quadrupole nuclei, ^{139}La and ^{27}Al, with a relatively high natural abundance. In particular, lanthanum has a big atomic number so we expect the hyperfine coupling to be sufficiently large. It would be interesting to try implementing the RDNMR technique on this platform as well.

We would like to thank K. Muraki of NTT Basic Research Laboratories for supplying high-quality wafers for this study. We thank K. Hashimoto, T. Tomimatsu, and T. Aono for helpful discussions and/or technical assistance. K.N. and Y.H. acknowledge support from the Graduate Program in Spintronics, Tohoku University. Y.H. acknowledges financial support from KAKENHI Grants No. 18H01811 and No. 15H05867. M.H.F. acknowledges financial support from KAKENHI Grant No. 17H02728.

[1] C. Beenakker and H. van Houten, Solid State Phys. **44**, 1 (1991).
[2] D. Loss and D. P. DiVincenzo, Phys. Rev. A **57**, 120 (1998).
[3] R. Hanson, L. P. Kouwenhoven, J. R. Petta, S. Tarucha, and L. M. K. Vandersypen, Rev. Mod. Phys. **79**, 1217 (2007).
[4] C. Bäuerle, D. C. Glattli, T. Meunier, F. Portier, P. Roche, P. Roulleau, S. Takada, and X. Waintal, Rep. Prog. Phys. **81**, 056503 (2018).
[5] D. A. Wharam, T. J. Thornton, R. Newbury, M. Pepper, H. Ahmed, J. E. F. Frost, D. G. Hasko, D. C. Peacock, D. A. Ritchie, and G. A. C. Jones, J. Phys. C: Solid State Phys. **21**, L209 (1988).
[6] B. J. van Wees, H. van Houten, C. W. J. Beenakker, J. G. Williamson, L. P. Kouwenhoven, D. van der Marel, and C. T. Foxon, Phys. Rev. Lett. **60**, 848 (1988).
[7] J. Miao, P. Charalambous, J. Kirz, and D. Sayre, Nature (London) **400**, 342 (1999).
[8] I. Robinson and R. Harder, Nat. Mater. **8**, 291 (2009).
[9] M. J. Hÿtch and A. M. Minor, MRS Bull. **39**, 138 (2014).
[10] D. Cooper, T. Denneulin, N. Bernier, A. Béché, and J.-L. Rouvière, Micron **80**, 145 (2016).
[11] T. M. G. Mohiuddin, A. Lombardo, R. R. Nair, A. Bonetti, G. Savini, R. Jalil, N. Bonini, D. M. Basko, C. Galiotis, N. Marzari, K. S. Novoselov, A. K. Geim, and A. C. Ferrari, Phys. Rev. B **79**, 205433 (2009).
[12] M. Huang, H. Yan, T. F. Heinz, and J. Hone, Nano Lett. **10**, 4074 (2010).
[13] C. Neumann, S. Reichardt, P. Venezuela, M. Drögeler, L. Banszerus, M. Schmitz, K. Watanabe, T. Taniguchi, F. Mauri,

B. Beschoten, S. V. Rotkin, and C. Stampfer, Nat. Commun. **6**, 8429 (2015).
[14] J. Zwanziger, U. Werner-Zwanziger, J. Shaw, and C. So, Solid State Nucl. Magn. Reson. **29**, 113 (2006).
[15] R. G. Shulman, B. J. Wyluda, and P. W. Anderson, Phys. Rev. **107**, 953 (1957).
[16] R. K. Sundfors, Phys. Rev. **177**, 1221 (1969).
[17] G. P. Flinn, R. T. Harley, M. J. Snelling, A. C. Tropper, and T. M. Kerr, Semicond. Sci. Technol. **5**, 533 (1990).
[18] D. J. Guerrier and R. T. Harley, Appl. Phys. Lett. **70**, 1739 (1997).
[19] E. A. Chekhovich, K. V. Kavokin, J. Puebla, A. B. Krysa, M. Hopkinson, A. D. Andreev, A. M. Sanchez, R. Beanland, M. S. Skolnick, and A. I. Tartakovskii, Nat. Nanotechnol. **7**, 646 (2012).
[20] R. M. Wood, D. Saha, L. A. McCarthy, J. T. Tokarski, G. D. Sanders, P. L. Kuhns, S. A. McGill, A. P. Reyes, J. L. Reno, C. J. Stanton, and C. R. Bowers, Phys. Rev. B **90**, 155317 (2014).
[21] A. Ulhaq, Q. Duan, E. Zallo, F. Ding, O. G. Schmidt, A. I. Tartakovskii, M. S. Skolnick, and E. A. Chekhovich, Phys. Rev. B **93**, 165306 (2016).
[22] M. Eickhoff, B. Lenzmann, D. Suter, S. E. Hayes, and A. D. Wieck, Phys. Rev. B **67**, 085308 (2003).
[23] M. S. Kuznetsova, K. Flisinski, I. Y. Gerlovin, M. Y. Petrov, I. V. Ignatiev, S. Y. Verbin, D. R. Yakovlev, D. Reuter, A. D. Wieck, and M. Bayer, Phys. Rev. B **89**, 125304 (2014).
[24] E. A. Chekhovich, M. Hopkinson, M. S. Skolnick, and A. I. Tartakovskii, Nat. Commun. **6**, 6348 (2015).
[25] C. Bulutay, E. A. Chekhovich, and A. I. Tartakovskii, Phys. Rev. B **90**, 205425 (2014).
[26] M. M. Willmering, Z. L. Ma, M. A. Jenkins, J. F. Conley, and S. E. Hayes, J. Am. Chem. Soc. **139**, 3930 (2017).
[27] J. H. Davies and I. A. Larkin, Phys. Rev. B **49**, 4800 (1994).
[28] I. A. Larkin, J. H. Davies, A. R. Long, and R. Cuscó, Phys. Rev. B **56**, 15242 (1997).
[29] A. R. Long, E. Skuras, S. Vallis, R. Cuscó, I. A. Larkin, J. H. Davies, and M. C. Holland, Phys. Rev. B **60**, 1964 (1999).
[30] G. Gervais, Resistively detected NMR in GaAs/AlGaAs, in *Electron Spin Resonance and Related Phenomena in Low-Dimensional Structures*, edited by M. Fanciulli (Springer, Berlin/Heidelberg, 2009), pp. 35–50.
[31] M. H. Fauzi, A. Singha, M. F. Sahdan, M. Takahashi, K. Sato, K. Nagase, B. Muralidharan, and Y. Hirayama, Phys. Rev. B **95**, 241404(R) (2017).
[32] See Supplemental Material at http://link.aps.org/supplemental/10.1103/PhysRevB.100.241301 for determining pinch-off voltages.
[33] A. Singha, M. H. Fauzi, Y. Hirayama, and B. Muralidharan, Phys. Rev. B **95**, 115416 (2017).
[34] A. Córcoles, C. J. B. Ford, M. Pepper, G. A. C. Jones, H. E. Beere, and D. A. Ritchie, Phys. Rev. B **80**, 115326 (2009).
[35] See Supplemental Material at http://link.aps.org/supplemental/10.1103/PhysRevB.100.241301 for the protocol timing diagram.
[36] See Supplemental Material at http://link.aps.org/supplemental/10.1103/PhysRevB.100.241301 for the other RDNMR subset data.
[37] See Supplemental Material at http://link.aps.org/supplemental/10.1103/PhysRevB.100.241301 for the calculation details.
[38] E. A. Chekhovich, I. M. Griffiths, M. S. Skolnick, H. Huang, S. F. Covre da Silva, X. Yuan, and A. Rastelli, Phys. Rev. B **97**, 235311 (2018).
[39] R. K. Sundfors, Phys. Rev. B **10**, 4244 (1974).
[40] A. K. Paravastu and J. A. Reimer, Phys. Rev. B **71**, 045215 (2005).
[41] G. Yusa, K. Muraki, K. Takashina, K. Hashimoto, and Y. Hirayama, Nature (London) **434**, 1001 (2005).
[42] T. Ota, G. Yusa, N. Kumada, S. Miyashita, and Y. Hirayama, Appl. Phys. Lett. **90**, 102118 (2007).
[43] See Supplemental Material at http://link.aps.org/supplemental/10.1103/PhysRevB.100.241301 for RDNMR signal from the bulk 2DEG.
[44] M. Kawamura, T. Yamashita, H. Takahashi, S. Masubuchi, Y. Hashimoto, S. Katsumoto, and T. Machida, Appl. Phys. Lett. **96**, 032102 (2010).
[45] J. Armstrong, N. Bloembergen, and D. Gill, Phys. Rev. Lett. **7**, 11 (1961).
[46] D. Gill and N. Bloembergen, Phys. Rev. **129**, 2398 (1963).
[47] E. Brun, R. J. Mahler, H. Mahon, and W. L. Pierce, Phys. Rev. **129**, 1965 (1963).
[48] K. A. Dumas, J. F. Soest, A. Sher, and E. M. Swiggard, Phys. Rev. B **20**, 4406 (1979).
[49] H. Yamaguchi, Semicond. Sci. Technol. **32**, 103003 (2017).
[50] K. Chida, M. Hashisaka, Y. Yamauchi, S. Nakamura, T. Arakawa, T. Machida, K. Kobayashi, and T. Ono, Phys. Rev. B **85**, 041309(R) (2012).
[51] N. Kumada, K. Muraki, and Y. Hirayama, Phys. Rev. Lett. **99**, 076805 (2007).
[52] A. M. Burke, O. Klochan, I. Farrer, D. A. Ritchie, A. R. Hamilton, and A. P. Micolich, Nano Lett. **12**, 4495 (2012).
[53] F. Bauer, J. Heyder, E. Schubert, D. Borowsky, D. Taubert, B. Bruognolo, D. Schuh, W. Wegscheider, J. von Delft, and S. Ludwig, Nature (London) **501**, 73 (2013).
[54] M. J. Iqbal, R. Levy, E. J. Koop, J. B. Dekker, J. P. de Jong, J. H. M. van der Velde, D. Reuter, A. D. Wieck, R. Aguado, Y. Meir, and C. H. van der Wal, Nature (London) **501**, 79 (2013).
[55] H. W. Liu, K. F. Yang, T. D. Mishima, M. B. Santos, and Y. Hirayama, Phys. Rev. B **82**, 241304(R) (2010).
[56] A. V. Shchepetilnikov, D. D. Frolov, Y. A. Nefyodov, I. V. Kukushkin, D. S. Smirnov, L. Tiemann, C. Reichl, W. Dietsche, and W. Wegscheider, Phys. Rev. B **94**, 241302(R) (2016).
[57] C. Mittag, M. Karalic, Z. Lei, C. Thomas, A. Tuaz, A. T. Hatke, G. C. Gardner, M. J. Manfra, T. Ihn, and K. Ensslin, Phys. Rev. B **100**, 075422 (2019).
[58] A. Jouan, G. Singh, E. Lesne, D. C. Vaz, M. Bibes, A. Barthélémy, C. Ulysse, D. Stornaiuolo, M. Salluzzo, and S. Hurand, arXiv:1903.1213.
[59] F. Zhang, P. Lv, Y. Zhang, S. Huang, C.-M. Wong, H.-M. Yau, X. Chen, Z. Wen, X. Jiang, C. Zeng, J. Hong, and J.-y. Dai, Phys. Rev. Lett. **122**, 257601 (2019).